A New Perspective and Explanation for the Formation of Plasmaspheric Shoulder Structures

Hua Zhang [1] Guangshai Peng[1] Chao Shen [2] Wu Yewen[1]

[1]Institute of Space Weather, Nanjing University of Information Science & Technology, Nanjing, China.

[2]Harbin Institute of Technology, Shen Zhen, China.

Correspondence: Hua Zhang (289534957@qq.com)

Abstract

Over the hours of 5-9 UT on 8 June 2001, the extreme ultraviolet (EUV) instrument onboard IMAGE satellite observed a shoulder-like formation in the morning sector and a post-noon plume-like structure. The plasmapause formation is simulated using the Test Particle Model (TPM), based on a drift motion theory, which reproduces various plasmapause structures and evolution of the shoulder feature. The analysis indicates that the Shoulder is created by sharp reduction and spatial non-uniform in the dawn-dusk convection electric field intensity. The TPM modeled event is found to develop an initial pre-dawn asymmetric bulge that becomes a shoulder as a result of increased "co-rotation" rate with increasing L-shell that is preceded by localized outward convection. The shoulder structure rotates sunward and develops into a single or double plume structure during an active time period in simulation.

1. Introduction

The plasmasphere is an important region in the inner magnetosphere, surrounding the Earth and extending to 5 Earth radii(Re), which contains dense(10-10000 cm^{-3}) and cold plasma (below 1ev). The plasmapause is formed by a superposition of corotation and convection electric field in the inner magnetosphere (Nishida, 1966; Chen and Wolf, 1972). The formation and size of plasmapause vary with a geomagnetic activity level. Generally, as the disturbance level increases, the plasmapause position moves closer to the Earth and of shape deviates from circle in the equatorial plane (Grebowsky, 1970). Atypical plasmapause structures, such as

‘bulge’ and plume, occur often in both whistler and in-situ data (Carpenter and Anderson, 1992). There are many theoretical research studies to explain the formation of plume (Grebowsky, 1970; Pierrard and Lemaire, 2004; Zhang et al., 2013), and Pierrard and Cabrera (2006) firstly simulated a double-plume , but did not explain the origin of second-plume.

The EUV instrument onboard IMAGE satellite was launched in March 2000, that provided a global perspective of the plasmasphere. Such as plume, finger, notch and shoulder, and so on, were observed by EUV (Sandel et al., 2001). One of plasmaspheric structures, shoulder, has been less studied in the previous papers than plume. However, the shoulder may play an important role in a loss mechanism for ring current (Burch et al., 2001). So, it is important to study the formation mechanism of the shoulder.

At present, there are no convincing explanations for the dynamic formation of shoulder. Goldstein et al.(2002) firstly proposed an explanation, based on the Magnetospheric Specification Model(MCM) simulation output, for the formation of shoulder. They proposed that the shoulder is created by a sudden decrease of dusk-dawn electric field. As the interplanetary magnetic field (IMF) turns northward from southward, it triggers anti-sunward flow of plasma in the predawn sector, to produce an asymmetric bulge called shoulder. Later, based on physical mechanism of interchange instability and a Kp-dependent E5D electric field model, Pierrard and Lemaire (2004) suggested that the shoulder is not the result of radial outflow of plasma, same as the presentation of Goldstein et al. (2002), but is inward plasma drift in post-midnight sector.

Then, scarce papers about dynamical formation of the shoulder are delivered than of the plume. In this paper, we used TPM to simulate dynamical formation of the shoulder, using Weimer’s statistical E-field (Weimer, 2001; Zhang et al., 2012), which is both spatially nonuniform and dynamically responsive to change geomagnetic and solar wind conditions. To drive the TPM model, several inputs are used: Dst, solar wind (SW) and interplanetary magnetic field (IMF) data sets. The authors make an attempt to propose a new convincing explanation for the formation

of the shoulder-like structure, different from the previous explanations.

2. Shoulder Observation

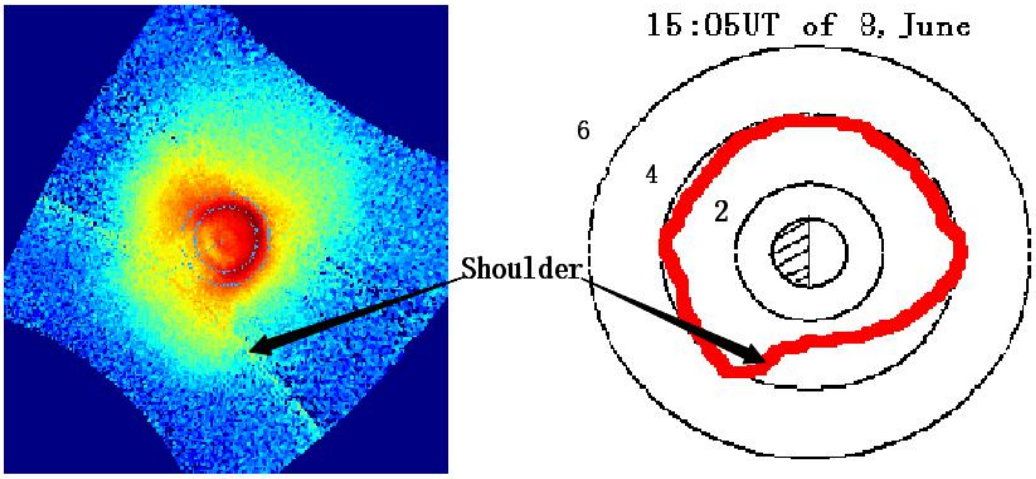

Figure1. Snapshot of plasmasphere (left panel) by EUV instrument, at 15:05 UT of 8 June 2001, Sunlight is an incident from the upper right. Earth is in the center of panels and shoulder is observed and labeled in the snapshot. The right panel is plasmapause that is extracted from the left plasmapheric image.

Figure 1 illustrates the shoulder-like structure, a sharp radial plasmaspheric structure about 1 RE radial extension, in the post-midnight sector, which was viewed by EUV imager onboard IMAGE satellite at 15:05 UT of 8 June 2001. The right panel illustrates the plasmapause extracted from the left panel in Figure 1. The outer boundary of plasmasphere is assumed to be 40% of maximum brightness of 30.4nm He^+ emission, where the intensity is the logarithm of the luminosity (Pierrard and Cabrera, 2006). Then, the shoulder-like is labeled and marked by arrows in the plot. Comparison of sequential observations with the simulation pictures, show that the shoulder structure corotating with the main plasmaspheric body can be seen in Figure 3, and is discussed in the next section. That means the outer edge of the shoulder corotates faster than the inner edge in development phase (Goldstein et al., 2002). Then, the shoulder moves eastward to the afternoon sector and evolves into the plume-like structure. Over the next hours, the outer body of plume flows sunward from noon sector, and results in the plume thinning out and disappearing (can see the simulation of Figure 3). In the next section, we take the case of 8 June 2001

observation as an example, to discuss the simulation of the Shoulder and the plume evolution based on the TPM method.

3. Simulation

In the region of plasmasphere occupied, charged particles are cold plasma (e.g. energy of particles is < 1eV). So, we can assume that plasma elements have only $\boldsymbol{E} \times \boldsymbol{B}/B^2$ drift motions (Li and Xu, 2005; Lejosne and Mozer, 2016). Here, the electric field intensity of E-model is superposition of convection and corotation electric field. The electric field plays a key role in plasma drift motion and the formation of plasmasphere (Pierrard et al., 2008). In the present paper, the Weimer's electric field (Weimer, 2001) is mapped into the magnetosphere along magnetic lines to model the magnetospheric convection electric field (Zhang et al., 2012), and T96 magnetic field to model the background magnetic field.

In the simulation, the calculation region is radial range of 2-7 Re and azimuthal span 0-359°. Dispersion by iso-spacing grids that correspond to the radial and azimuthal steps are equal to 0.1Re and 1° respectively, in the magnetic equatorial plane. Ten particles are placed into each grid, so particle density is proportional to L^{-1} which is not consistent with the actual density in a saturation state (close to true density presumably is proportional to L^{-4}), but is adequate to study the evolution of plasmaspheric morphology using a skeleton map of particles during a substorm period. The TMP runs 3 days under the low activity condition to obtain the boundary conditions for the simulation.

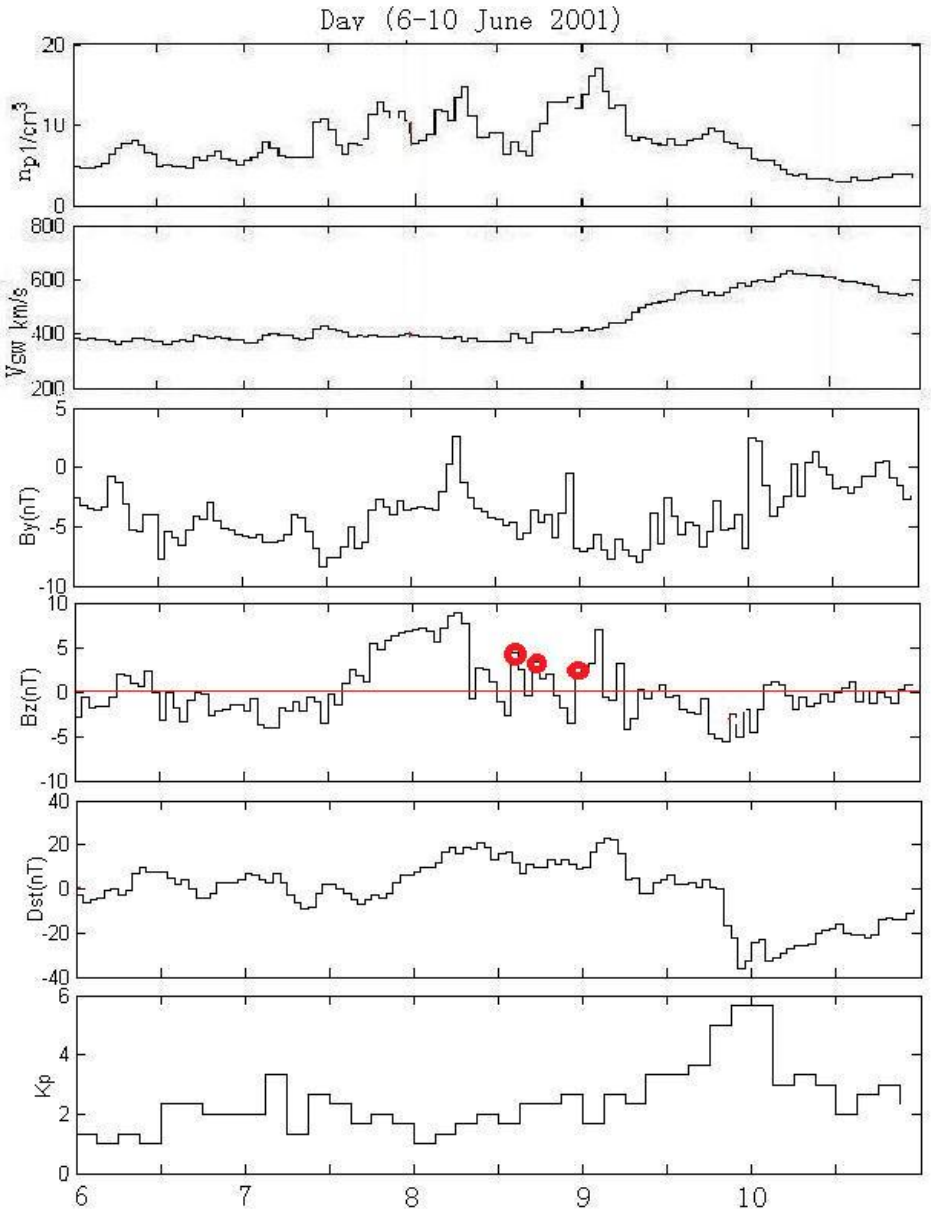

Figure 2. Input parameters of the TPM model, the variation of the By and Bz component of the IMF, the Dst index and Kp index, on 6 -10 June 2001, is a typical substorm case.

The paper presents the case of 8-9 June 2001, to study the evolution of the shoulder and propose a hypothetical explanation produced by TPM simulation. During the geomagnetic substorm, all the TPM inputs are available. IMF and Solar Wind data are available in ACE satellite data center, and Dst index can be seen in World Data center for Geomagnetism, Kyoto. Fig.2 shows the By, Bz components of the IMF, the Dst index and the geomagnetic activity index Kp, observed from 6 to 10 June 2001. This is a typical substorm case where the Kp index gradually increases up to 5+ and then decreases. The TPM runs with

3-minute time resolution from 6 June at 00:00 UT to 10 June at 12:00 UT. The results of simulation are shown in Fig.3, whose corresponding times are labeled on the title of each panel. The simulated plasmapause is a skeleton which consists of continuous particle distribution. Comparison of TPM simulation (black body) and EUV observation (red line) in Fig.3 indicates that the simulated plasmapause positions correspond generally rather favorable with the EUV observations. The results of EUV observation show that the plasmapause is seldom smooth or irregular, due to the fluctuations in plasmapause region caused by successive particles injection during a disturbance period (Goldstein et al., 2002; Gallagher et al., 2005), in agreement with previous whistler observations (Carpenter and Anderson, 1992). In contrast, the simulation of plasmapauses by TPM is more smooth. So, observations and simulations are not identical, due to deviation in the extraction of the boundary from EUV image and optical contamination of the image (Sandel et al., 2001; Zhang et al., 2013) and the limitation in the TPM model and the unrealistic Weimer electric field model. .

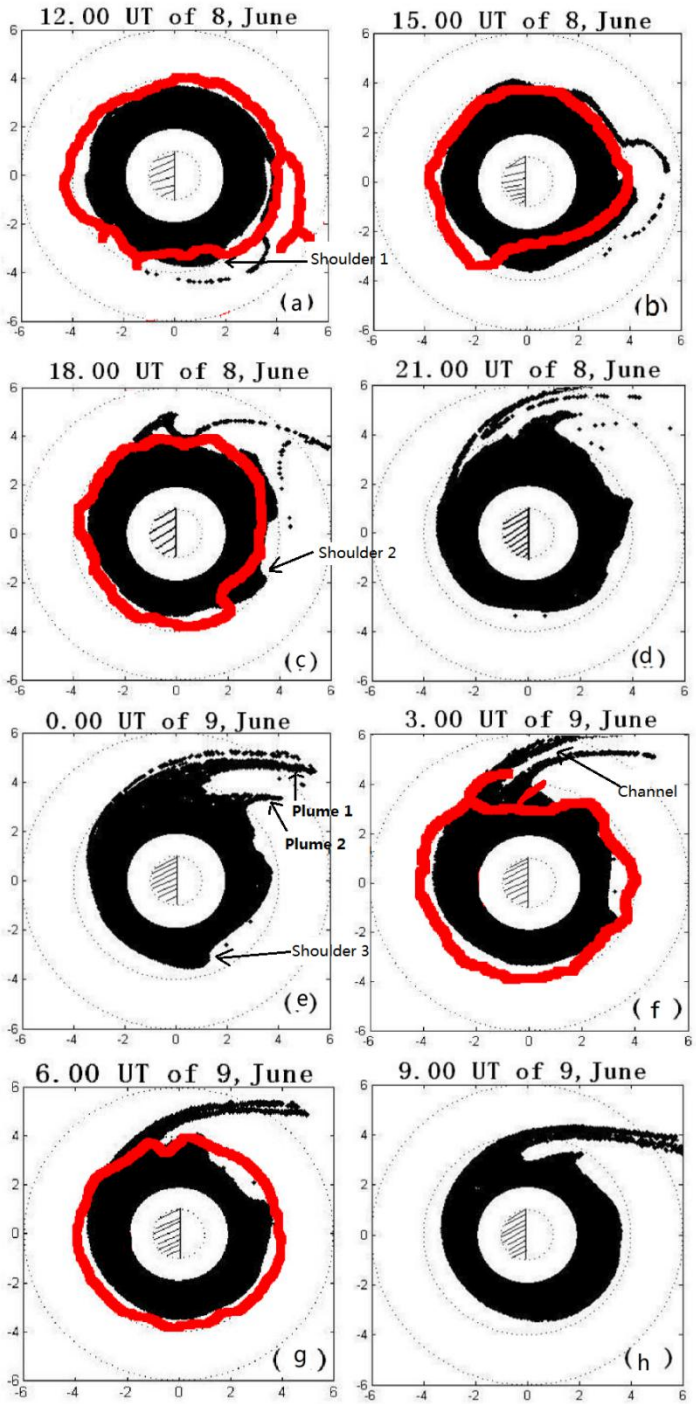

128

129 **Figure 3. The simulation of plasmaspheric morphology compared with EUV/IMAGE observation in the**
130 **geomagnetic equatorial plane on 8 - 9 June 2001. The red irregular curves indicate plasmapause**
131 **observation by EUV/IMAGE. Black contours are the plasmasphere simulated by the TPM model. White**
132 **contours are the main plasmasphere (located at 1-2 Re region). The dotted circles on the panels**
133 **correspond to L=1, 2, 4 and 6.**

134

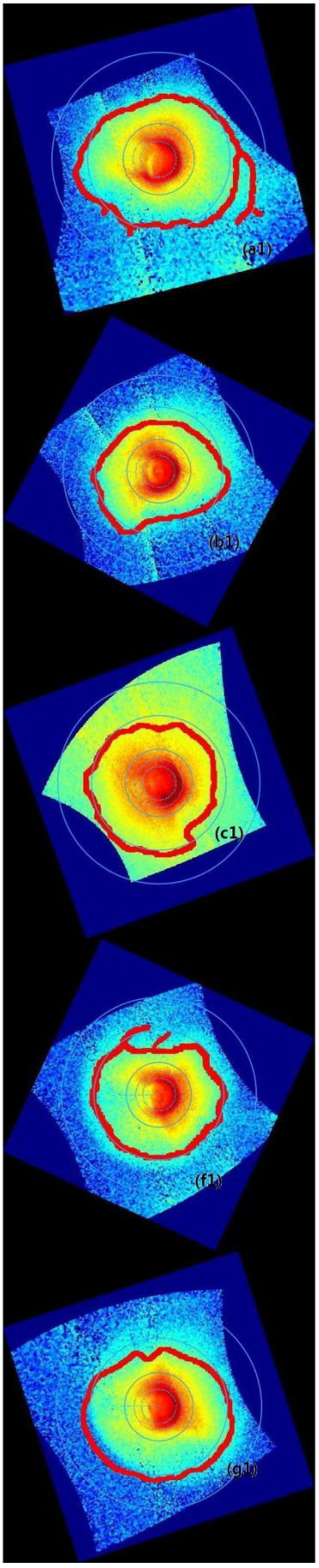
(a1)
(b1)
(c1)
(f1)
(g1)

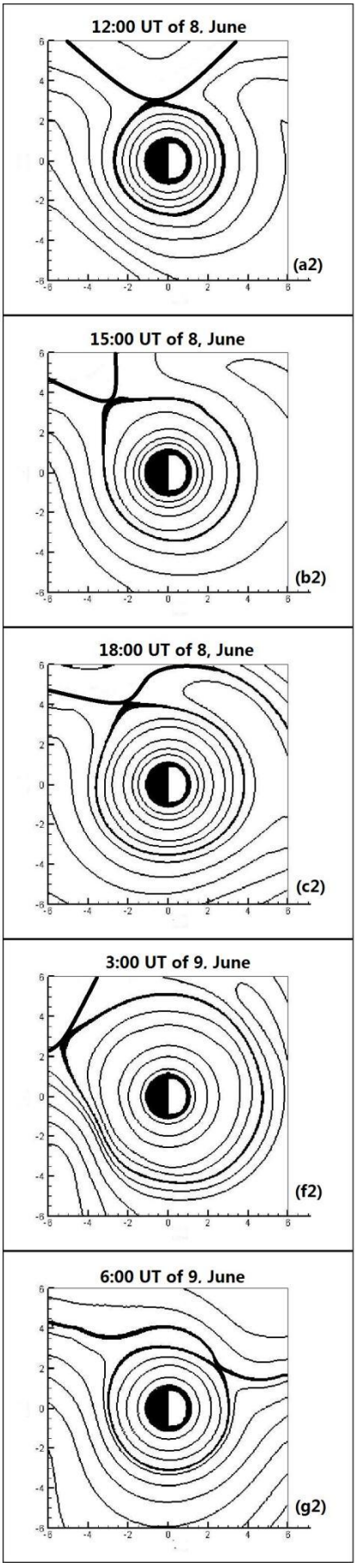
12:00 UT of 8. June
(a2)
15:00 UT of 8, June
(b2)
18:00 UT of 8, June
(c2)
3:00 UT of 9. June
(f2)
6:00 UT of 9. June
(g2)

135

Figure 4. The subscript of panels correspond to Figure 3. The left column of panels show original observation results by EUV/IMAGE, the blue circles on the panels correspond to L=1, 2, 4 and 6. The right column of panels show equipotential lines in the equatorial plane, the last closed equipotential (LCE) is the bold black curve.

Panels of Fig.3(a) - (h) illustrate the plasmasphere obtained on the interval of from at 12:00 UT on 8 June to at 09:00 UT on 9 June in 2001 with snapshots every three hours. Figure4 illustrates original observations by EUV/IMAGE and equipotential lines in the equatorial plane. When the Kp index increased, the last closed equipotential shits closer to the Earth. The results of the simulation show the evolution and development of the features of the plasmapause, like shoulders and plumes. One can see that the plasmapause is closer to the Earth in the predawn sector. The reason is the increase of rotation velocity resulting in plasmapause of inward flow in the predawn sector (Pierrard and Cabrera, 2006; Verbanac et al., 2018). At 15:05 UT of 8 June, the TMP simulation captures an infant shoulder-like structure in panel Fig.3 (b), and then corotates with the plasmasphere body moved eastward and further reproduces a mature shoulder formation in Fig.3(c). The overall agreement between TPM simulation and EUV observed is quite well, but the TPM shoulder is located ~1.5 hours earlier in magnetic local time (MLT) that probably originated from the convection electric field model (Goldstein et al., 2002; Pierrard and Cabrera, 2005; Zhang et al., 2013).

The EUV observation illustrated in Fig.3 (f) shows that a plume is indeed observed in the afternoon or dusk sector. The results of the simulation also reproduce the formation and the evolution of the plumes, which derives from the shoulder structure in this case, illustrated in panels of Fig.3 (d)-(f). The simulation shows that the shoulders generate in the post-midnight sector (Verbanac et al., 2018), and then rotates eastward around the Earth to the afternoon sector (Goldstein et al., 2002). When the level of geomagnetic activity increases, the plasma element in the shoulder around the outer plasmasphere would convect outward and then into the dayside magnetopause (Li and Xu, 2005; Pierrard et al., 2008), and produce the plasmaspheric plume structure. The shoulder1 firstly arises on Fig.3(a) in the morning sector (at 12

166 UT, 8 June 2001), and then corotates with the main body of the plasmasphere to the
167 afternoon sector on Fig.3(c)(at 18 UT, 8 June 2001). During this period, the Kp index
168 increases to 3+ from 1 (see in Fig.2), and magnetosphere convection is slightly
169 enhanced that triggers plasma elements in the shoulder1 doing sunward convection,
170 then produces the plume1 at 21 UT on 8 June 2001 (see in Fig.3(d)). The mature
171 shoulder2, illustrated in Fig.3(b), corotates eastward with the Earth to the
172 afternoon-dusk sector. During the period of 0-3 UT on June 9, the Kp index gradually
173 increases up to 5+, indicating that magnetospheric convection is enhanced and the
174 convective electric field increases. The infantile plume2, illustrated in the panel of
175 Fig.3(e), derives from outflow of plasma elements in the shoulder2, and evolves into
176 the mature plume2 in Fig.3(f). Later, the double-plumes formation that is extended
177 from the plasmapause to the magnetosphere, is presented in the simulation results in
178 panels of Figs.3 (e)-(f).

179 The cavity in between the double plumes, or between plumes and the main body
180 of plasmasphere, may be responsible for the formation of channel and notch structures
181 (Gallagher et al., 2005). The base and the westward edge of the plume are connected
182 with the main body of plasmasphere. Moreover, there is a cavity topology, a
183 low-density region, between the tail structure of the plasmasphere and the main body
184 of plasmasphere. That is the channel structure of the plasmasphere. The plume
185 corotates with the Earth, becomes thinner, and finally disappeared (Li and Xu, 2005).
186 The results of simulation reproduce the channel structure in Fig.3(f). Gallagher et al.
187 (2005) proposes that notches and channels share the same origin, which derive from a
188 low-density cavity in the dusk region during recovery at the base of the plasmaspheric
189 plume. The absence of notch structure in this simulation event is due to the fact that
190 the potential structure does not cause the inward flow of plasma in the afternoon
191 sector, and the low disturbance time is maintaining for not long enough.

192 By contrastive analysis on between Fig.2 and Fig.3, the formation of the
193 shoulder is produced during the intensity of the convection electric field suddenly
194 decrease (Goldstein et al., 2002; Pierrard and Lemaire, 2004), when IMF sudden turns
195 northward from southward. There are three shoulders reproduced during this substorm

period, depicted in panels of Fig.3 (b)-(g). The time of the shoulder appearance is labeled by three red circles in Fig.2, at 14:00 UT, 17:00 UT, 23:00 UT on 8 June respectively. At that moment, the Bz component of the IMF turns northward. But not all of the times, the Bz component of the IMF that turns northward could produce the shoulder structure. One can see that no shoulders were reproduced in the results of the simulation, at 02:00 UT, 05:00 UT, and 08:00 UT on 9 June 2001 respectively. The Bz value of southward component must be less than the previous 24-hours mean value. The intensity of the convection electric field is greater than the previous 24-hours level. So the last closed equipotential line (LCE) would be closer to the Earth and result in plasmapause of inward flow in the predawn sector (Zhang et al., 2013).

4. **Discussion**

The physical explanation of shoulder formation is not yet understood. In the present section, we use the case of Figure 1 as an example to investigate the physical mechanism of shoulder formation based on the TPM model. Fourteen test particles are placed in the range of $2.5 \leq L \leq 3.8$, initial position located at 12:00 MLT, space step takes 0.1Re, and then trace these particles' motion. Outputs are the trajectory (see in Fig.5(a)) and the rotation rate (see in Fig.5(b)) of these test particles corresponding to given magnetic local time illustrated in the bottom of Fig.5.

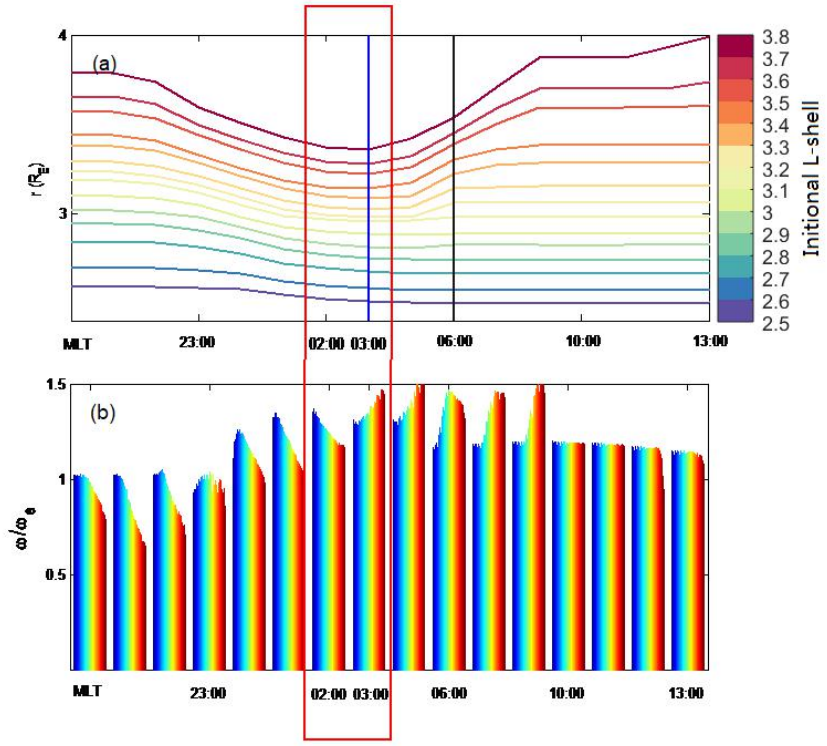

Figure 5. The trajectory (upper plot) and the rotation rate (bottom plot) of 14 test particles corresponding to MLT (location-dependent) during a substorm. The legend indicates fourteen test particles of various initial L-shell. The day is 8 June 2001.

The top panel shows that the outer part of plasmasphere (L>3.3 Re) drifts inward before 02 MLT, and moves outward (could reach up to 3.9 Re position) in the predawn sector (after 03:00MLT sector) (Verbanac et al., 2018). The radial motion of inner plasmasphere (L<3.3) is negligible. The shoulder is forming across 03-06 MLT region (between blue vertical line and black vertical line in Figure 5(a)). The outermost particle moves outward 0.7 Re, and the fourth particle moves outward 0.45 Re, from 03:00 MLT to 08:00 MLT. So, the shoulder has a sharp eastern edge about 0.2Re~0.3Re in radial extension and across a narrow 3-5 hours MLT region. Goldstein et al.(2002) proposed the shoulder formation by an outward radial motion of plasma in a narrow range and in the morning sector. The simulation of this paper verifies the conclusions of Goldstein (2002) and Verbanac (2018).

The lower panel shows the corotational angular velocity of test particles in the range of 2.5 < L< 4.0. The simulation results suggest that plasma element in

plasmasphere region rotation speed varies significantly with radial distance (Galvan, 2010). The inner part of plasmasphere rotates faster than its outer part before 02:00 MLT sector, vice versa in a range of in the 03:00-08:00 MLT sector [Lejosne and Mozer, 2016]. The previous researchers analyzed the EUV observation and proposed the shoulder structure has MLT sharpening in the angular direction. It indicates that the outer edge of the shoulder rotates faster than the inner edge, resulting in steepening of the MLT-profile of the shoulder (Goldstein et al., 2002). The lower panel shows, with the increase of L, the rotation rate of the plasmasphere tends to slightly decrease on the dusk side and obviously increase on the dawn side.

Fig. 5 indicates, in the region of 21:00 - 23:00:00 MLT, that the rotation rate is about corotation in the inner plasmasphere (L<3), but is the interval of 70% - 90% of corotation in the outer plasmasphere (L>3). The rotational value decreases with the increase of L [Galvan et al., 2010]. Gallagher et al. (2005) investigates the drift rate of notches in the geomagnetic quite phase, and the results show that the average rotation rate of plasmasphere is about 90% of the corotational rate, in agreement with the results of Lejosne and Mozer (2016). When the plasma elements rotate to the region of 23:00 - 02:00 MLT, rotation rate in the outer plasmasphere reaches ~ 130% of corotation, and in the inner plasmasphere is also close to the corotation rate. The results show that the rotation rate of plasmasphere is overall increasing in the region. In addition, the plasma elements in the outer plasmasphere rotate faster than the inner plasmasphere in this region. The Fig.5(b) shows that rotation rate in the outer plasmasphere highly reaches ~ 140% of corotation, and rotation rate in the inner plasmasphere is close to 110% of corotation. So, we propose that the physical mechanism of the shoulder formation is plasma extrusion of outer plasmasphere in the predawn sector, due to outer plasmasphere both drifts radial outward and rotates faster. In the present paper, the results show that the rotation rates of simulation are higher than the observations, and not consistent with Huang et al. (2011) and Galvan et al. (2010). The first reason is that this is a substorm case, so the convection of magnetosphere is greater than the previous study articles of the geomagnetic quiet case. (Galvan et al., 2010; Huang et al., 2011; Verbanac et al., 2018). The second

reason is that the Weimer electric field model is larger in practice, which results in a larger total electric field value in calculation (Goldstein et al., 2002; Pierrard et al., 2008).

The dawn-dusk asymmetry of convective electric field is caused by the terminal conductivity gradient of the ionosphere. The subrotation of the ionosphere drives the subrotation of the plasmasphere, and the plasmaspheric drift is correlated with the phase of geomagnetic storm (Burch et al., 2004). The convection electric field of Weimer (2001) is obvious dawn-dusk asymmetry, that causes a smaller increase on the dawnside and a lager decrease on the duskside, indicating that the subrotational effect of the plasmasphere is modulated by field-aligned current changes and conductance variations (Liemohn et al., 2004). The asymmetry of potential pattern causes the sunward convection in the magnetospheric night-side to be larger than that in the morning side, resulting in the subcorotational flow in the dark side. (Gallagher et al., 2005).

5. Conclusion

In this paper, we simulated the case of substorm on 8 June 2001 to investigate the physical mechanism of the shoulder formation based on TPM model that utilizes Weimer's electric field and the drift motion theory. We use the E-model and the B-model that are qusi-static background field and global averages. So, the results of simulation have some deviations with EUV observation. But, we have satisfactorily reproduced the evolution and development of the features of the plasmapause, like the shoulders and plumes. And then, the physical mechanism of the shoulder formation has been investigated.

The formation of shoulder is associated with IMF northward turning in the predawn sector. And the physical mechanism of shoulder formation is the result of plasma extrusion in the predawn sector, caused by the fact that outer plasmasphere drifts radially outward and rotates faster. The corotation rate in midnight sector decreases with the increasing L-shell, while it increases in pre-dawn sector. So, the shoulder

forms across in the 03-06 MLT region.

The formation and evolution of plume and channel have also been reproduced in this case. One can see single or double plumes appear in the dusk or afternoon sector, then become thinner with time, and finally disappear.

In this model, we do not consider the refilling process of the ionosphere. In the future work, the refilling process should be considered, and we expect to obtain more reasonable results. And also, the physical mechanisms of plasmaspheric features observed by EUV/IMAGE, like notch or channel, also are to be investigated by TPM model in future work underway.

Code availability: The code of electric field model is provided by the professor D. R. Weimer, and the code of geomagnetic model can download from website (https://ccmc.gsfc.nasa.gov/modelweb/magnetos/data-based/Geopack_2005.html).

Data availability: Geomagnetic indexes and ACE satellite data can come from the website (http://wdc.kugi.kyoto-u.ac.jp/wdc/Sec3.html). The dataset of EUV/IMAGE could be downloaded from the website (http://euv.lpl.arizona.edu/euv/).

Author contributions: Zhang H. conceptualized the project and wrote the original draft of the paper. Peng G. S. modified the Figures and coded the Fortran program. Shen C. supervised the project, and reviewed and edited the paper. Wu Yewen gives some suggestions and draws Figure 4 for the paper.

Competing interests: The authors declare that they have no conflict of interest.

Acknowledgment: The author thanks the professor D. R. Weimer, who provided the code of Weimer's electric field model. We thanks for two anonymous referees and the editor. This work was supported by the National Key R&D Program of China (2018YFC1407304), the Natural Science Foundation of Jiangsu Province (BK20170952), the National Natural Science Foundation of China grant

(No.41874190), and the Stable support projects of institutes for basic scientific research (A131901W14, A131902W03).

References

Burch, J. L., Mende, S. B., Mitchell, D. G., Moore, T. E. , Pollock, C. J., Reinisch, B. W., Sandel, B. R., Fuselier, S. A. , and Gallagher D. L.: Views of Earth's magnetosphere with the IMAGE satellite, Science, 291, 691-624, doi: 10.1126/science.291.5504.619, 2001.

Carpenter, D. L. and Anderson, R. R.: An ISEE/Whistler model of equatorial electron density in the magnetosphere, J. Geophys. Res., 97, 1097-1108, doi:10.1029/91JA015481992, 1992.

Chen, A. J. and Wolf, R.A. : Effects on the plasmasphere of a time-varying convection electric field, Planet. Space Sci., 20, 483-509, doi: 10.1016/0032-0633(72)90080-3, 1972.

Gallagher, D. L., Adrian, M. L. and Liemohn, M. W.: Origin and evolution of deep plasmaspheric notches, J. Geophys. Res., 110, A09201, doi:10.1029/2004JA010906, 2005.

Galvan, D. A., Moldwin, M. B., Sandel, B. R., and Crowley, G. : On the cause of plasmaspheric rotation variability: IMAGE EUV observation, J. Geophys. Res., 115, A01214, doi:10.1029/ 2009JA014321, 2010.

Goldstein, J., Spiro,R. W., Reiff, P. H., Wolf, R. A., Sandel, B. R., Freeman, J. W., and Lambour, R. L.: IMF-driven overshielding electric field and the origin of the plasmaspheric shoulder of May 24, 2000, Geophys. Res. Lett., 29(16), 1819, doi:10.1029/2001GL014534, 2002.

Grebowsky, J. M.: Model study of plasmapause motion, J. Geophys. Res., 75, 4329-4333, doi:10.1029/JA075i022p04329, 1970.

Huang Y., Xu, R. L., Shen, C., and Zhao H.: Rotation of the Earth's plasmasphere at different radial distances, Adv. Space. Res., 48, 1167-1171, doi: 10.1016/j.asr.2011.05.028, 2011.

Lejosne, S., and Mozer, F. S. : Van Allen Probe measurements of the electric drift

351 $\boldsymbol{E}\times\boldsymbol{B}/B^2$ at Arecibo's L=1.4 field line coordinate, Geophys. Res. Lett., 43, 6768-6774,
352 doi: 10.1002/2016GL069875, 2016.
353 Li, L., and Xu, R. L.: Model of the evolution of the plasmasphere during a
354 geomagnetic storm, Adv. Space. Res., 36, 1895-1899. doi: 10.1016/j.asr.2003.10.057,
355 2005.
356 Nishida A.: Formation of plasmapause, or magnetospheric plasma knee, by the
357 combined action of magnetospheric convection and plasma escape from the tail, J.
358 Geophys. Res., 71, 5669-5679, doi:10.1029/JZ071i023p05669, 1966.
359 Pierrard V., and Lemaire, J. F.: Development of shoulders and plumes in the frame of
360 the interchange instability mechanism for plamapause formation, Geophys. Res. Lett.,
361 31, L05809, doi:10.1029/2003GL018919, 2004.
362 Pierrard, V., and Cabrera, J.: Comparisons between EUV/IMAGE observations and
363 numerical simulations of the plasmapause formation, Annales Geophysicae, 23,
364 2635-2646, doi:10.5194/angeo-23-2635-2005, 2005.
365 Pierrard, V., and Cabrera, J.: Dynamical simulations of plasmapause deformations,
366 Space.Sci.Res, 122, 119-126, doi: 10.1007/s11214-006-5670-3, 2006.
367 Pierrard, V., Khazanov, G. V., Cebrera, J., and Lemaire, J.: Influence of the convection
368 electric field models on predicted plasmapause positions during magnetic storms. J.
369 Geophys. Res. 113, A08212, doi:10.1029/2007JA012612, 2008.
370 Sandel, B. R., King, R. A., Forrester, W. T., Gallagher, D. L., Broadfoot, A. L., and
371 Curtis, C. C.: Initial results from the IMAGE extreme ultraviolet imager, Geophys.
372 Res. Lett., 28, 1439, doi: 10.1029/2001GL012885, 2001.
373 Verbanac, G., Bandic, M., Pierrard, V., and Cho, J.: MLT plasmapause characteristics:
374 Comparison between THEMIS observations and numerical simulations. J. Geophys.
375 Res: Space physics, 123, 2000-2007, doi:10.1002/2017JA024573, 2018.
376 Weimer, D. R.: An improved model of ionospheric electric potentials including
377 substorm perturbations and application to the Geospace Environment Modeling
378 November 24, 1996, event., J. Geophys. Res., 106, 407-416,
379 doi:10.1029/2000JA000604, 2001.
380 Zhang, H., Xu, R. L., Zhao, H., and Shen, C.: The characteristics of the model of

Weimer's electric field within the magnetosphere., Chinese J. Geophys. 55, 36-45, doi: 10.6038/j.isnn.0001-5733.2012.01.004, 2012.

Zhang, H., Xu, R. L., Shen, C., and Zhao, H.: The simulation of the plasmaspheric morphology during a magnetospheric disturbance event, Chin J. Geophys, 56, 731-737, doi:10.6038/cjg 20130302, 2013.